Four-Electrode System for the Measurement of Biological Tissue Conductivity at ELF and ULF

Erika Pittella, *Member, IEEE*, Vanni Lopresto, Stefano Pisa, *Senior Member, IEEE*, and Emanuele Piuzzi, *Member, IEEE*

***Abstract*—This article presents the metrological characterization of a four-electrode compact system able to measure the dielectric properties of biological tissues at extremely low and ultralow frequencies, where data available from the literature are very limited. The cell constant *k* of the system, together with its expanded uncertainty, is found measuring different saline solutions of known conductivity. Since the cell constant plays a key role in the determination of tissue dielectric properties, it has been further verified through tests on other saline solutions, containing a different type of solute, confirming the accuracy of the system. In particular, results on a saline solution with a given molar concentration of KCl and on a physiological solution (Eurospital 0.9% NaCl) show that the system maximum relative error is lower than 3.3%. Therefore, it can be concluded that the system correctly measures the conductivity in saline solutions, and the parameter *k* can be properly used for the measurement of dielectric properties of biological tissues. As an application example, the system is used to perform measurements on bovine liver. Liver conductivity measurements show a constant behavior as a function of frequency in the examined range. Furthermore, the comparison of our results with the few data found in the literature at low frequencies shows good agreement. These observations point out the feasibility and convenience of the proposed method for the measurement of the conductivity at very low frequency.**

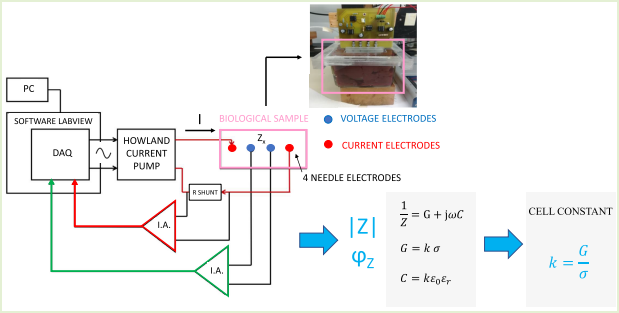

***Index Terms*— Biological tissues, dielectric properties, measurement system calibration, measurement uncertainty, saline solutions.**

I. Introduction

KNOWLEDGE of the dielectric properties of biological tissues at frequencies lower than 10 Hz is useful in specific operating environments, such as magnetic resonance imaging (MRI) equipment rooms [1], [2]. The movement of the operator near an MR imaging device occurs in a condition of nonhomogeneous static magnetic field. This scenario is equivalent to a stationary subject in a slowly time-varying homogeneous magnetic field, whose frequency range varies between 0.1 and a few Hz [3]. Other application scenarios for which tissue dielectric property knowledge at low frequencies is necessary are, for example, electroporation [4], [5] and electrochemotherapy [6], [7]. Both techniques rely on the uses of micropulse and nanopulse series that cause the opening of cell membrane channels, allowing the transport within the target cells of specific substances, such as drugs [8]. The effect of these pulses is the induction of an EM field whose frequency range spans between 0 Hz and a few MHz (micropulses) or GHz (nanopulses) [9], [10]. The dosimetric tools necessary to evaluate the induced field in MR, electroporation, and electrochemotherapy would benefit from the knowledge of low-frequency complex permittivity values, as also evidenced in recent recommendations [11], [12].

A first major investigation into the electrical properties of biological tissues has been carried out by Schwan [13], who, in a pioneering paper, highlighted the dispersive behavior of tissues in a wide-frequency range, pointing out electrode polarization as a major problem. Further studies were conducted between the 1970s and 1980s of the last century [14], [15], [16]. In particular, Hart [14] and [15] discussed, in detail, precautions that must be taken in the choice of the measuring-circuit parameters and frequency range to avoid the introduction of artifacts into the resulting permittivity spectra. A critical review of the electrical properties of tissues and other biological materials is presented by Foster and

Manuscript received 5 June 2024; accepted 7 June 2024. Date of publication 19 June 2024; date of current version 1 August 2024. The associate editor coordinating the review of this article and approving it for publication was Dr. Chirasree Roychaudhuri. *(Corresponding author: Erika Pittella.)*

Erika Pittella, Stefano Pisa, and Emanuele Piuzzi are with the Department of Information Engineering, Electronics and Telecommunications, Sapienza University of Rome, 00185 Rome, Italy (e-mail: erika.pittella@uniroma1.it).

Vanni Lopresto is with Italian National Agency for New Technologies, Energy and Sustainable Economic Development, Casaccia Research Center, 00123 Rome, Italy.

Digital Object Identifier 10.1109/JSEN.2024.3413953

TABLE I
STATE-OF-THE-ART COMPARATIVE TABLE

Paper	Measurement type	Limits
[13]	Biological tissue dispersive behavior in a wide frequency range	Electrode polarization is a major problem
[17]	Dielectric spectrometer able to measure body tissue characteristics with jelly-type silver/silver-chloride electrodes	Time domain measurement No metrological characterization
[18]	Systematic studies on many biological tissues (human and animal)	For most tissues absence of data for f lower than 10 Hz Frequency band: 10 Hz to 20 GHz
[19]	Ex-vivo measurements on human liver with the four-electrode measurement technique	Absence of data below 1 kHz Frequency band: 1 kHz to 400 kHz
[20]	Ex-vivo measurements on human liver 4-terminal technique	Absence of data for f lower than 10 Hz Frequency band: 10 Hz up to 100 MHz

Schwan [16], which summarizes the classical principles underlying dielectric relaxation and includes a summary of the most significant advances in the theory of polarization effects. Singh et al. [17] proposed the development of a dielectric spectrometer able to measure the relative permittivity and the dielectric loss of body tissues at low frequency, limiting the polarization problem. The authors tested a variety of electrodes on different types of samples, finding that jelly electrodes were very satisfactory for this kind of measurement. However, this study was performed in the time domain, requiring a quite complex system comprising a voltage transient generator, a capacitor bridge, an amplifier, an A/D converter, memory banks, and a microprocessor to perform the signal processing. Moreover, no metrological characterization was performed. Gabriel et al. [18] used three experimental techniques based on automatic swept-frequency generators and impedance analyzers; these techniques have allowed dielectric property evaluation for both human and animal biological tissues. Nevertheless, for frequencies below 10 Hz, data are scarce or completely absent for most tissues. In [19] and [20], the four-electrode measurement technique was used to evaluate human liver dielectric properties through ex vivo measurements. An experimental analysis was conducted in the presence and absence of tumors in the 1–400-kHz [19] and 10-Hz–100-MHz [20] frequency ranges. A comparative table, summarizing the state of the art, is shown in Table I.

Considering the state of the art, it appears evident that data at frequencies lower than 10 Hz are very few or totally absent. However, as previously highlighted, the knowledge of the electrical properties of biological tissues at very low frequencies is required for many biomedical applications, because they can provide insight into the basic mechanisms that rule the interaction of electric fields with tissues. The absence of these data can be explained by the presence of relevant measurement systematic errors at the lower frequencies.

With regards to commercial systems, in [21], the modular Alpha-A system is presented. This dielectric/impedance measurement system works at different available frequency ranges: in particular, depending on the "Mainframe Types," it can span from 3 μHz to 40 MHz. The ZG4 extension test interface, recommended for dielectric samples, is required for four-electrode measurements to partly compensate for electrode–sample interface polarization or contact impedance effects.

Another commercial device able to measure the dielectric properties in the desired frequency range is the Zurich Instruments MFIA, a digital impedance analyzer, and precision LCR meter that allows impedance measurements in the frequency range from 1 mHz to 500 kHz (extendible to 5 MHz) [22]. This instrument can measure dielectric properties over a wide-frequency range down to 1 mHz and over a broad range of impedance values up to 1 TΩ.

These commercial systems present an accuracy for the impedance measurement of 0.2%–10% for Alpha A and 0.05%–10% for the Zurich Instruments MFIA, depending on the impedance value and frequency. However, they also present a very high instrument cost, on the order of tens of thousands of Euros. Moreover, in order to measure the complex permittivity of tissues with these commercial instruments, it is necessary to design, build, and calibrate a proper measurement cell, such as the open ended coaxial probe largely used at high frequency [23], [24], connecting the tissue to the instrument interface.

In a previous paper [25], the authors focused on the design and characterization of a low-cost and compact system for biological tissue dielectric property measurements between 0.1 Hz and 1 kHz. In particular, accuracy tests were conducted in [25], measuring discrete component (resistances and capacitors) impedances (both magnitude and phase). Measurement accuracy of the four-terminal system was verified by comparing the measured values of discrete components of known value with measurements performed with a reference multimeter and an LCR meter. From the results achieved in [25], a relative error for the impedance magnitude of around 0.3% was obtained, while the phase maximum error was equal to 0.15°.

The aim of this article is to develop a low-cost system for the measurement of biological tissue dielectric properties at ELF and ULF frequencies, where data available from the literature are almost absent. In particular, efforts are targeted toward the conductivity measurement, trying to keep the error related to the temperature effect under control. Emphasis is given to conductivity alone, because available literature data suggest that the complex permittivity of tissues at very low frequencies is dominated by the imaginary part (i.e., the one associated with tissue conductivity), with tissue permittivity playing a minor role. In particular, the measurement system calibration in saline solutions is performed, along with test measurements on ex vivo bovine liver. In Section II, the measurement system configuration is shown, and the system elements are described. Sections III and IV present the measurement system calibration in saline solutions and its verification on other saline solutions, respectively. Section V shows results on bovine liver. Finally, the conclusions are drawn in Section VI.

II. MEASUREMENT SYSTEM

A. Block Scheme, Circuit Schematic, and Layout

The measurement of the biological tissue impedance, from which the dielectric properties can be extracted, relies on the

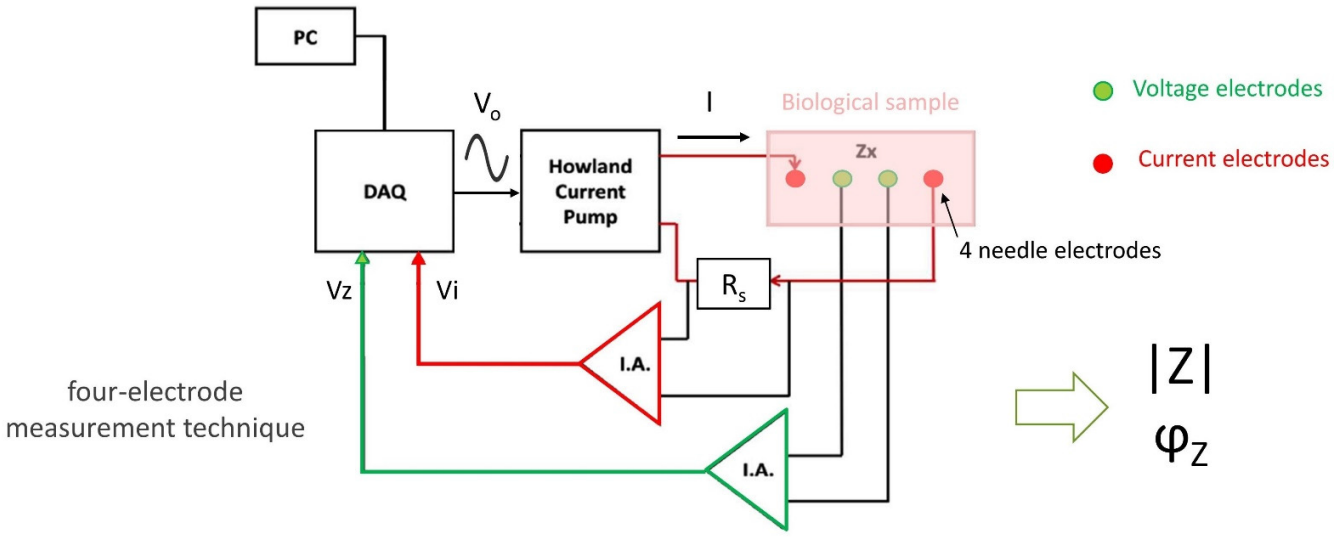

Fig. 1. Block diagram of the measurement system.

"I–V method" [26]. To limit electrode polarization effects, the four-electrode technique was used [27], [28].

The block scheme of the measurement system is depicted in Fig. 1. A LabVIEW[1] virtual instrument (VI) controls the output signal (V_o) of the DAQ board (NI-USB 6351, National Instruments, Austin, TX, USA), which is a sinusoidal voltage, whose frequency is adjustable by the program [25]. The same VI acquires the voltage across the voltage electrodes, amplified by an instrumentation amplifier (IA), and the amplified voltage drop across the shunt resistor (R_s in the figure).

The V_o voltage signal is sent to a Howland current pump circuit input [29], which supplies a current injected into the tissue by the two external current electrodes (custom Ag–AgCl needle electrodes [25]). The value of the Howland current pump transconductance is fixed by the gain resistance, chosen equal to 1 kΩ, to provide a current of 1-mA peak injected into the load when the pump is driven by a sinusoidal signal with a peak amplitude of 1 V [29]. The voltage generated in the tissue is sensed by two inner sensing electrodes and is read by the IA, with high input impedance.

The two DAQ board acquired signals are processed by the VI, which extracts the magnitude and phase of the complex impedance (Z_x in Fig. 1).

The printed circuit board (PCB) design was implemented with the open-source software Eagle, a graphical editor for designing schematics, and PCBs. First, the schematic of the circuit was designed (shown in Fig. 2). Below is a brief description of the elements present in the schematic.

1) Two AD620 IAs are used to read at high impedance and amplify the voltage between the two voltmetric electrodes and the voltage drop on the shunt resistor, placed in series with the load to be analyzed.
2) An improved Howland current pump [29] is used to obtain the currents of the desired value. The pump is built around the TL082 operational amplifier, and the conversion factor (transconductance) has been set through the 1-kΩ resistor.
3) A shunt resistance equal to 10 Ω is used to measure the injected current.
4) A voltage converter (TC7662B) has been added to feed the PCB-integrated circuits. It allows to obtain −5 V starting from the +5 V supplied by the DAQ board; for this purpose, it is necessary to insert a 10-μF electrolytic capacitor.
5) Two further electrolytic capacitors are added to the positive and negative supply rails for voltage stabilization.
6) A terminal block is added for the connection to the DAQ board.
7) Four connectors are present to connect the electrodes.

The obtained circuit layout is shown in Fig. 3.

B. Mechanical Stability Tests and Sample Holder Optimization

Before carrying out the metrological characterization of the system with standard saline solutions, it was necessary to perform tests to verify the mechanical stability of the measurement system, considering that some effort is required to insert the needle electrodes inside the biological tissue sample. In particular, the geometry of the four linearly arranged needle electrodes should not be altered due to the insertion in the material under test. To this end, the first step was fixing the PCB on a positioner that allowed controlling the penetration depth of the electrodes with a spatial resolution of about 1 mm. Subsequently, the electrodes were glued, using a hot glue gun, on a plastic support to avoid any unwanted shifts (vertical or horizontal) as much as possible. Then, tests were carried out to evaluate the mechanical stability of the measuring system using a sample of chicken breast as a test medium (see Fig. 4). The choice of this type of tissue was made, because it is readily available and presents a higher stiffness as compared with bovine liver. In this way, if the system is mechanically stable, it can be assumed that this will also be true in the case of bovine liver samples.

Eight measurement tests were carried out on chicken breast samples. The distances between the electrodes (D1, D2, and D3 in Fig. 4) were measured before and after insertion

[1]Trademarked.

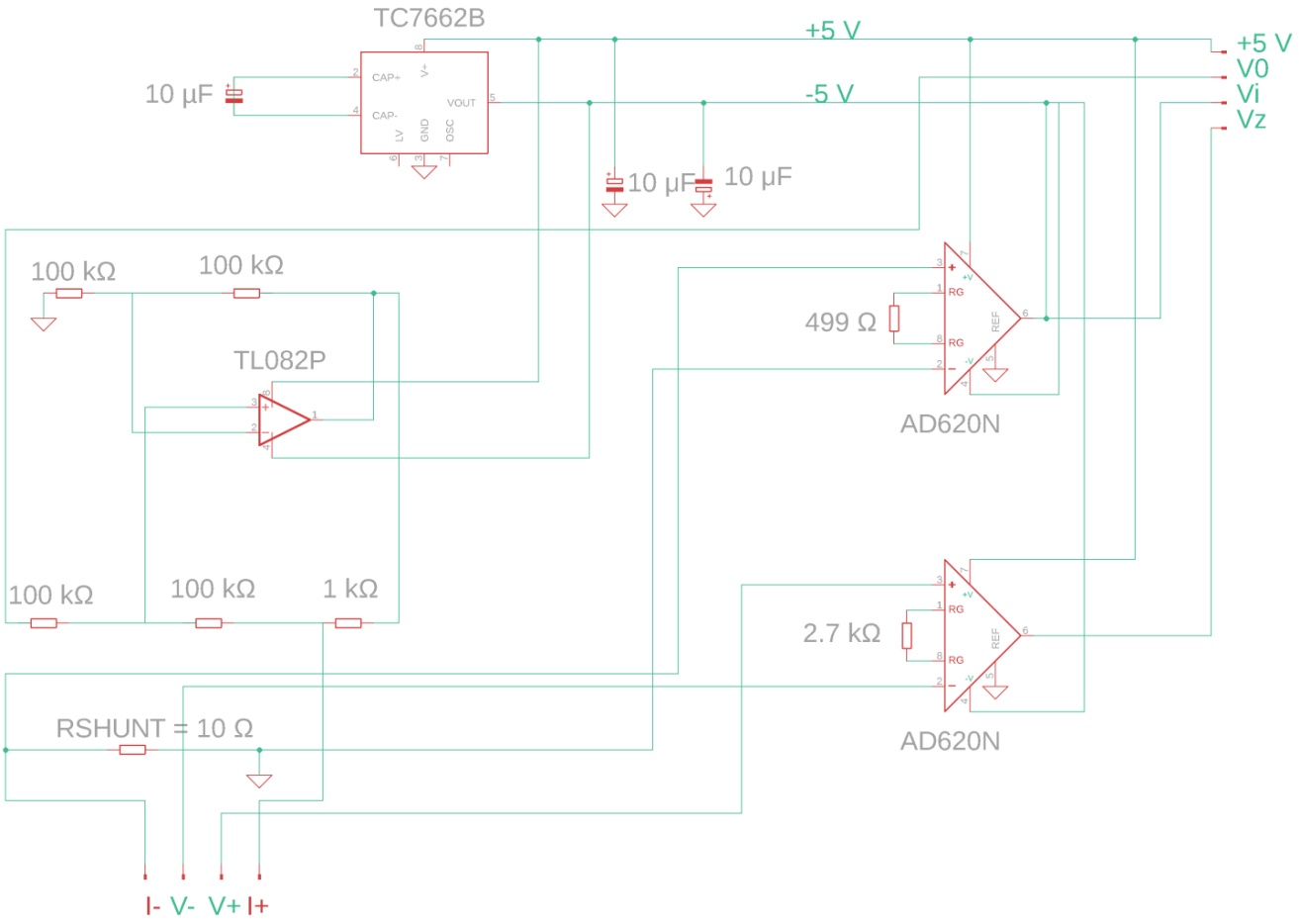

Fig. 2. Circuit schematic.

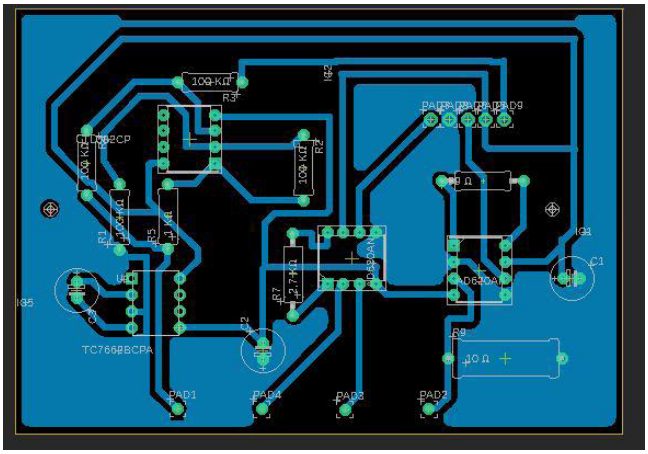

Fig. 3. Layout of the circuit designed with Eagle.

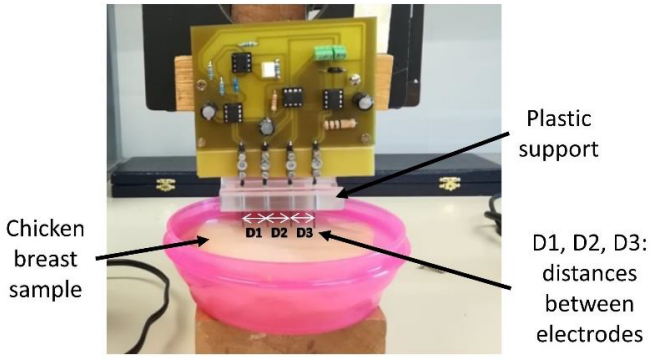

Fig. 4. Mechanical stability test on a chicken breast sample.

(penetration depth equal to 1.6 cm) into the tissue to quantify any displacements. The obtained results show that, in the worst case, a variation of the order of one-tenth of a millimeter was achieved, which can be attributed in part to the uncertainty of the interelectrode distance measurements. Indeed, these measurements were carried out with the 20th caliper (maximum error ± 0.05 mm) paying particular attention not to bend the electrodes.

Finally, the exposed electrode surface was also checked, which remained unchanged, since it was blocked by two constraints: 1) the fixing of the electrodes with hot glue to the plastic base and 2) the terminal block with which the electrodes are in electrical contact with the PCB.

Once the mechanical stability of the measuring system was verified, some supplementary tests were carried out for the choice of the container to be used for the calibration of the measuring system in saline solutions.

In particular, four containers were tested and filled with a given saline solution. Three repeated measurements of conductance at 1 kHz were carried out to evaluate how much the dimensions of the container influenced the measured value.

The saline solution used for this type of experiment was the Eurospital 0.9% NaCl physiological solution, a standard solution that is easy to find and low cost. These measurements

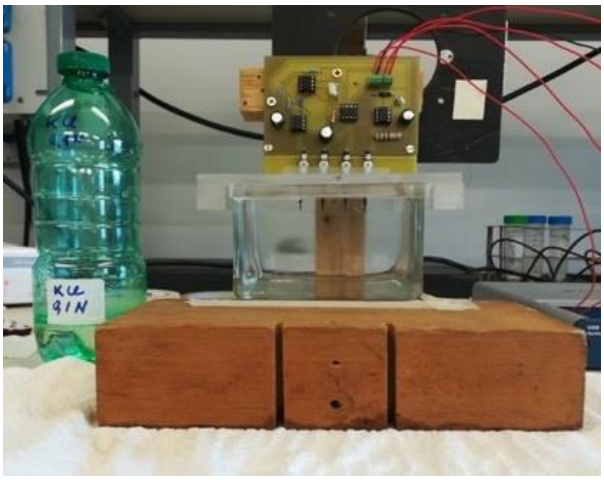

Fig. 5. Configuration of the compact measurement system for calibration with standard saline solutions.

allowed us to select the container in which the edge effect had a minor impact on the measurement result. The final dimensions are 9.5 × 6 × 7.5 cm.

III. Measurement System Calibration in Saline Solutions

When a sinusoidal voltage is applied to the biological tissue, the impedance Z is given by the ratio between the phasor associated with this voltage and the one representing the current that flows inside the tissue $Z = (V/I)$. Alternatively, the admittance value may be taken into consideration, equal to $Y = (1/Z) = G + j\omega C$, where G is the conductance (S) and C is the capacitance (F). In the considered setup, G and C depend on the geometry of the measurement system and the dielectric properties of the tissues, as reported in the following equations:

$$G = k\sigma \tag{1}$$

$$C = k\varepsilon_0\varepsilon_r \tag{2}$$

where k (m) is the cell constant (dependent on the geometry of the system), σ is the tissue conductivity (S/m), ε_r is the tissue relative permittivity, and $\varepsilon_0 = 8.85 \cdot 10^{-12}$ F/m is the vacuum permittivity.

The key role played by the cell constant k in the study of the dielectric properties of biological tissues is evident. To obtain its value, taking as a reference the recent studies by Gabriel et al. [30] and Laufer et al. [19], a calibration was carried out with three saline solutions with different molar concentrations (M = mol/L) of potassium chloride (KCl). These solutions were chosen, because their conductivity value is well known from the literature, allowing to compute $k = G/\sigma$.

Fig. 5 displays the configuration of the measurement system for calibration with saline solutions.

A. Used Saline Solutions

The standard saline solutions used for calibration of the measuring system are as follows:

1) 0.1-M KCl: 7.455 g of solute in 1 L of deionized water;
2) 0.01-M KCl: 0.7455 g of solute in 1 L of deionized water;
3) 0.001-M KCl: 0.07455 g of solute in 1 L of deionized water.

These saline solutions were prepared using the Radwag precision balance model AS 220.3Y, which has a maximum error of 0.1 mg [31].

For each solution, ten repeated conductance measurements were carried out for the following reference frequencies: 0.1 Hz, 1 Hz, 10 Hz, 100 Hz, and 1 kHz. In particular, measurements at the lowest frequency had the aim of evaluating the possible presence of distortions in the waveforms detected by the sensing electrodes.

Temperature control was performed using the Hart Scientific 1521 thermometer (Hart Scientific Inc., now Fluke Corporation, American Fork, UT, USA) with a maximum error of 0.005 °C [32], [33]. The temperature was measured at the beginning and at the end of each measurement, to keep under control possible variations that could have significantly influenced the measurements.

The advantages of using these saline solutions rely on the following: 1) the availability of conductivity values as a function of temperature in the literature and 2) their pure resistive behavior at frequencies lower than 1 MHz.

Therefore, once the conductance G value is measured and the conductivity σ value is obtained from the literature, the calculation of the cell constant k is straightforward

$$k = \frac{G}{\sigma}. \tag{3}$$

TABLE II
Results of the First Analyzed Solution (0.1-M KCl)

	G MEASUREMENT @1 kHz				
	G (S)	σ_T (S/m)	T_i (°C)	T_f (°C)	k (m)
	0.1152	1.2208	22.24	22.25	0.0944
	0.1153	1.2210	22.25	22.25	0.0944
	0.1150	1.2215	22.26	22.27	0.0941
	0.1147	1.2222	22.30	22.30	0.0939
	0.1152	1.2222	22.30	22.32	0.0942
	0.1149	1.2220	22.29	22.30	0.0940
	0.1149	1.2227	22.32	22.33	0.0939
	0.1148	1.2227	22.32	22.33	0.0939
	0.1147	1.2224	22.31	22.33	0.0938
	0.1146	1.2232	22.34	22.35	0.0938
MEAN	0.1149	1.2221	22.29	22.30	0.0940
STANDARD DEVIATION	0.0003	0.0008	0.033	0.036	0.0003

B. Cell Constant Evaluation

For the first analyzed solution (0.1-M KCl), the peak amplitude of the voltage supplied at the input was set equal to 1 V. The values obtained in the ten repeated measurements performed at the frequency of 1 kHz are shown in Table II. In particular, G is the measured conductance, and $\sigma_\mathbf{T}$ is the conductivity, as a function of the measured average temperature, calculated from the literature [34]. Temperature values were registered both at the beginning (T_i) and the end (T_f) of each measurement. Using this information, an average temperature was computed, and a conductivity value ($\sigma_\mathbf{T}$) was extrapolated.

Starting from the measured voltage V_{meas} and the voltage read on the shunt resistor V_{ref}, the LabVIEW function "Tone

TABLE III
AVERAGE VALUES OF THE PARAMETERS CALCULATED AT THE VARIOUS FREQUENCIES FOR THE 0.1-M KCL SOLUTION

	KCl 0.1 M				
	f (Hz)	G_{AVE} (S)	T_{AVE} (°C)	σ_{AVE} (S/m)	k_{AVE} (m)
	1000	0.114932	22.30	1.222056	0.09405
	100	0.114436	22.39	1.224185	0.09348
	10	0.114473	22.49	1.226664	0.09332
	1	0.114759	22.62	1.2298856	0.09331
	0.1	0.115991	22.82	1.234392	0.09396
MEAN		0.114918	22.523	1.22743	0.09362
SEM		0.00009	0.064	0.00035	0.00006
CV		0.08%	0.29%	0.03%	0.07%

TABLE IV
AVERAGE VALUES OF THE PARAMETERS CALCULATED AT THE VARIOUS FREQUENCIES FOR THE 0.01-M KCL SOLUTION

	KCl 0.01 M				
	f (Hz)	G_{AVE} (S)	T_{AVE} (°C)	σ_{AVE} (S/m)	k_{AVE} (m)
	1000	0.013115	21.0	0.130670	0.10037
	100	0.013132	21.05	0.130630	0.10053
	10	0.013131	21.13	0.130856	0.10034
	1	0.013223	21.36	0.131442	0.10059
	0.1	0.013370	21.88	0.132844	0.10064
MEAN		0.01319	21.30	0.13129	0.10049
SEM		0.00002	0.11	0.00014	0.00010
CV		0.12 %	0.5 %	0.10 %	0.10 %

TABLE V
AVERAGE VALUES OF THE PARAMETERS CALCULATED AT THE VARIOUS FREQUENCIES FOR THE 0.001-M KCL SOLUTION

	KCl 0.001 M				
	f (Hz)	G_{AVE} (S)	T_{AVE} (°C)	σ_{AVE} (S/m)	k_{AVE} (m)
	1000	0.001323	21.33	0.013666	0.09681
	100	0.001328	21.51	0.013701	0.09692
	10	0.001340	21.79	0.013757	0.09738
	1	0.001351	22.24	0.013872	0.09737
	0.1	0.001351	22.55	0.013959	0.09680
MEAN		0.001339	21.88	0.01379	0.09706
SEM		0.000002	0.16	0.00001	0.00010
CV		0.12 %	0.7 %	0.04 %	0.11 %

Measurements" is used. This function is able to provide amplitude, phase, and frequency of the two voltages V_{meas} and V_{ref}. From these data, the magnitude $|Z|$ and phase φ_Z of the impedance are computed. Using the "Polar to Complex" and "Complex to Re/Im" LabVIEW functions, the real part (resistance R) and the imaginary part (reactance X) are obtained. Therefore, the conductance (G) values are then obtained through the following formula:

$$G = \frac{R}{R^2 + X^2}. \tag{4}$$

From the measured G and extrapolated $\sigma_{\mathbf{T}}$ values, the cell constant k was computed for each repeated measurement. Finally, the mean and standard deviation were calculated for each of the parameters. The same method was applied for the other frequencies of interest (0.1, 1, 10, and 100 Hz).

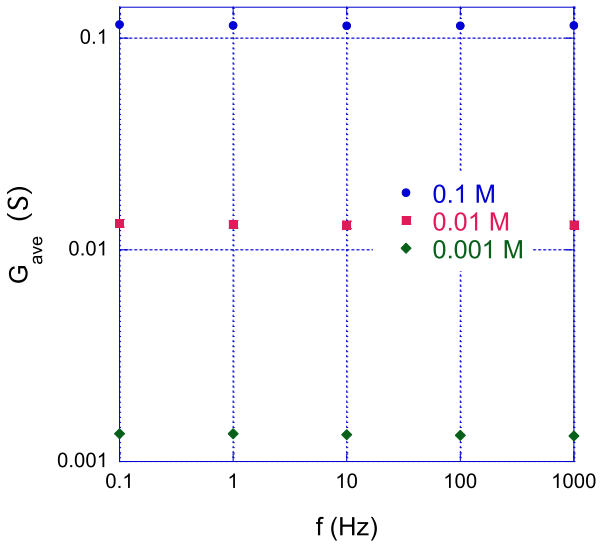

Fig. 6. Frequency behavior of the conductance for the considered standard saline solutions (M = mol/L).

In processing the data, the average of the means and the associated uncertainty expressed through the standard error of the mean (SEM) were calculated (see Table III). By dividing the uncertainty by the mean of the means, it was also possible to obtain the value of the coefficient of variation (CV). The same procedure was used for the other two saline solutions. Therefore, the final tables including the average values of the parameters of interest are shown in Tables IV and V.

Considering the different solutions separately, it is evident that the average conductance values, shown in Fig. 6 for each molar concentration, do not reveal a significant dispersion in frequency. Statistically, this is confirmed by the reduced value of the standard error of the average.

The same result was, therefore, achieved for the cell constant k, which shows, for each solution, a constant value as the frequency varies. Also, in this case, the uncertainty, associated with the average of the average of the cell constants (mean of k_{AVE}), assumes, in all three cases, a very low value, which indicates the cell constant final value reliability, extrapolated from each standard saline solution.

The next step was to calculate a single cell constant for the measurement system, which will allow, at a later stage, the evaluation of the dielectric properties of the biological tissue. In particular, the average is performed on the three different average cell constants extracted from the same number of standard solutions. The relative standard error (SEM) is also computed (see Table VI).

C. Cell Constant Uncertainty Evaluation

The cell constant is a quantity determined by an indirect measurement. Therefore, for the calculation of the associated combined uncertainty, it is necessary to consider the standard uncertainties for the input quantities (conductance and conductivity) on which it depends. In detail, conductance (G) and conductivity (σ) are characterized, respectively, by a type-A uncertainty (u_G) and by a type-B uncertainty (u_σ).

The standard uncertainty u_G is equal to the standard error (SEM) of the mean conductance calculated for each examined

TABLE VI
AVERAGE VALUE OF THE CELL CONSTANT

	MOLAR CONCENTRATION KCl	k (m)		
N	M (mol/L)	k_{AVE}	SEM_{AVE}	CV (%)
10	0.1	0.09363	0.00006	1.51
10	0.01	0.10050	0.00010	0.34
10	0.001	0.09706	0.00010	0.58
		$k_{AVE,TOT}$	$SEM_{AVE,TOT}$	CV
		0.097	0.00009	1.41

TABLE VII
CONDUCTIVITY MEASUREMENT FOR THE 1-M KCL SOLUTION

	σ MEASUREMENTS 1 m KCl @1 kHz				
	σ_{MEAS} (S/m)	σ_{THEO} (S/m)	e_r (%)	T_i (°C)	T_f (°C)
	9.4314	9.7465	3.23	19.09	19.10
	9.4679	9.7446	2.84	19.08	19.22
	9.4879	9.7651	2.84	19.19	19.21
	9.4733	9.7689	3.03	19.21	19.28
	9.4260	9.7820	3.64	19.28	19.32
	9.4797	9.7894	3.16	19.32	19.42
	9.4110	9.8081	4.05	19.42	19.42
	9.5308	9.8081	2.83	19.42	19.42
	9.5472	9.8081	2.66	19.42	19.53
	9.4728	9.8287	3.62	19.53	19.54
MEAN	9.473	9.785	3.19	19.30	19.35
STANDARD DEVIATION	0.043	0.028	0.45	0.15	0.14

saline solution. The type-B uncertainty, u_σ, is directly linked to the measurement uncertainty of the scales with which the solutions were prepared. In fact, using the definition of molar mass (g/mol), it is possible to calculate, starting from the uncertainty of the scales, the uncertainty with which the molar concentration of a given solution was quantified.

Considering the relationship of direct proportionality between the electrical conductivity of a saline solution and the molar concentration of the electrolyte, it is possible to obtain the measurement uncertainty of the conductivity u_σ.

To obtain the uncertainty of the cell constant, it is necessary to apply the combined standard uncertainty formula to (3), resulting in

$$u(k_i) = |k_i| \sqrt{\frac{u_G^2}{|G|^2} + \frac{u_\sigma^2}{|\sigma|^2}} \tag{5}$$

where the index i represents the ith standard saline solution examined, and conductance and conductivity measurements are supposed to be uncorrelated in terms of uncertainty. This hypothesis can be made, since G was obtained from impedance measurements and is characterized by a type-A uncertainty, while σ was obtained from literature formulas and is characterized by a type-B uncertainty, linked to the measurement uncertainty of the scale used to prepare the solutions, as described previously. This calculation is performed for all three cell constants extrapolated from the same number of standard solutions examined.

Once the uncertainties of the three average cell constants are determined, the total standard uncertainty of the cell constant of the measurement system is expressed as follows:

$$u(k) = \frac{\sqrt{\sum_{i=1}^{3} (uKi)^2}}{3} = 0.00008 \text{ m}. \tag{6}$$

Assuming a Gaussian distribution for the indirect measurement, and expressing the final result with a 95% confidence level, the expanded uncertainty $U(k)$ can be determined as follows:

$$U(k) = 2 \cdot 0.00008 \text{ m} = 0.00016 \text{ m}. \tag{7}$$

Therefore, the final cell constant of the measurement system, also considering the expanded uncertainty, is equal to $k = (0.09706 \pm 0.00016)$ m. In Section IV, this value for k will be verified through tests on other saline solutions before measurements on bovine liver, verifying the accuracy of the system.

IV. VERIFICATION OF THE K PARAMETER WITH OTHER SALINE SOLUTIONS

Once the value of the cell constant was obtained, the next step was to verify its reliability by performing conductivity measurements in different saline solutions.

In the first stage of the examination, a KCl solution with the following molal concentration (mol/kg) was chosen:

1) 1-M KCl: 1 mol (74.55 g) of solute in 1 kg of deionized water.

For this saline solution, ten repeated measurements of conductance were carried out for each of the following measurement frequencies: 1 kHz, 100 Hz, 10 Hz, 1 Hz, and 0.1 Hz. The conductivity in these cases was computed using the cell constant obtained from the measurement system characterization in standard solutions.

In each test, the temperature was checked both at the beginning and at the end of the measurement. Similar to the standard solutions, also in this case, the tabulated values of conductivity as a function of the temperature are available [32].

The data interpolation curve as a function of the temperature is known from the literature [34], and it is

$$\sigma = a + bT + cT^2 + dT^3 \tag{8}$$

where σ indicates the conductivity (S/m) and T the temperature (°C). Terms a, b, c, and d vary according to the molal concentration of the solution. Accordingly, the solution is characterized by its relevant equation through which the conductivity value can be assessed at the temperature of interest. This value was then compared with the conductivity calculated by the four-electrode measurement system.

The values measured over the ten tests, performed at the frequency of 1 kHz, are shown in Table VII. By comparing the values of conductivity obtained with the two methodologies (σ_{MEAS}, i.e., the conductivity obtained from the conductance G, measured by the four-electrode system, and the relevant cell constant, and σ_{TH}, i.e., the conductivity obtained from the data interpolation curve derived from the literature), the relative percentage error was calculated, considering σ_{TH} as a reference value. In the final analysis, the mean and standard

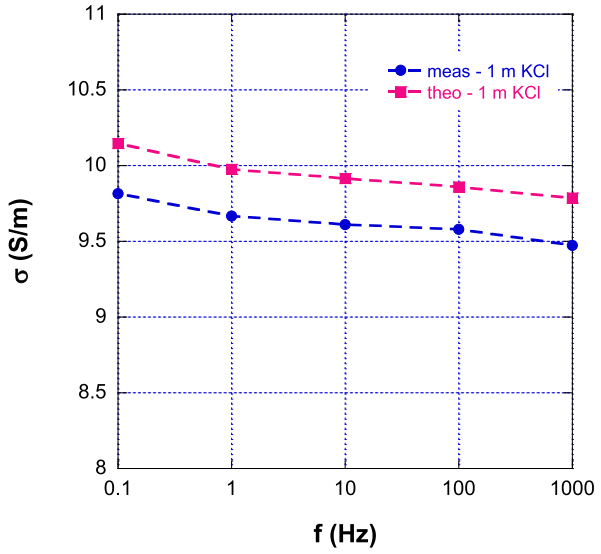

Fig. 7. Frequency behavior of the measured and theoretical conductance for the considered saline solution.

deviation on the ten repeated tests were calculated for each tabulated parameter. The same procedure was applied to the other frequencies. The calculated average conductivity remains constant as the frequency varies. The average relative errors range from a minimum of 2.9% to a maximum of 3.3%. Fig. 7 shows the trend of the average measured and theoretical conductivity as a function of the frequency in logarithmic scale.

To expand the investigation, it was decided to carry out an experimental test using a solution containing a different type of solute. Among the various options, the Eurospital 0.9% NaCl physiological solution was chosen for the advantages listed above (see Section III). The obtained conductivity values were compared with data taken from [19]. In this case, the calculated relative percentage error shows values between 1.2% and 3.1%.

The maximum relative error achieved from the tests for verifying the accuracy of the measurement system performed both in saline solutions with molal concentrations of KCl different from those used in the calibration step and in physiological solution is lower than 3.3%. Therefore, it can be concluded that the four-electrode system correctly measures the conductivity in saline solutions, and that the cell constant parameter k, obtained by the calibration measurements in standard saline solutions (see Table VI), can be used for the measurement of dielectric properties of biological tissues.

By considering the maximum relative error of the impedance magnitude and the maximum error for the phase estimated in [25], it is possible to determine theoretically the standard uncertainty u_G, starting from $G = Re(Y) = |Y|\cos(\varphi_Y)$, and applying the uncertainty propagation formula. Then, since $\sigma = (G/k)$, the standard uncertainty of σ is equal to

$$u_\sigma = |\sigma| \sqrt{\frac{u_G^2}{|G|^2} + \frac{u_k^2}{|\mathrm{k}|^2}}. \tag{9}$$

As an example, for the 1-M KCl, the value of the measured average conductance is $G_{\text{ave}} = 0.9194246$ S; thus, the conductivity with its expanded uncertainty with a coverage factor of 2 is $\sigma = (9.474 \pm 0.036)$ S/m; for the second solute, i.e., the Eurospital 0.9% NaCl, $\sigma = (1.3157 \pm 0.0050)$ S/m is obtained, with a relative percentage error of 0.4% in both cases. This theoretical uncertainty evaluation confirms that the expected uncertainty for conductivity measurements is definitely acceptable for biological tissue characterization.

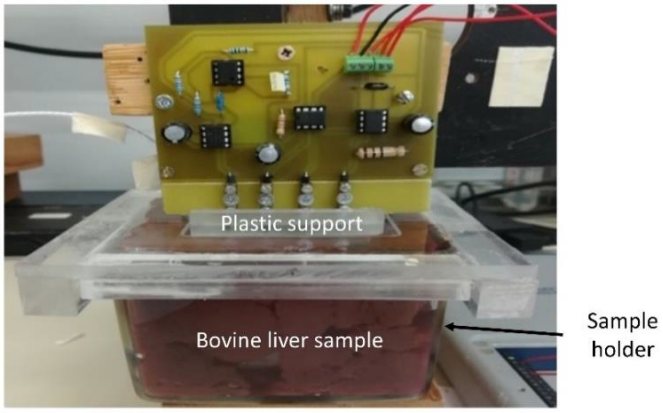

Fig. 8. Picture of the setup for measurements in ex vivo bovine liver.

Comparing the proposed compact measurement system with available commercial systems, it is apparent the indisputable advantage of the former, due to it being compact and, above all, of very low cost.

Focusing on accuracy, the datasheets of the commercial systems contain accuracy data on impedance measurements [21], [22]. Our system accuracy on impedance measurements was studied and reported in [25]. In particular, from the achieved results, a maximum relative error of around 0.3% was assessed for the measurement of impedance magnitude with respect to the reference values, while a maximum error equal to 0.15° was assessed for phase measurement. These values are comparable with or only slightly worse than those of the much more expensive commercial instruments Alpha A (magnitude: 0.2% and phase: 0.06°) and Zurich Instruments MFIA (magnitude: 0.05% and phase: 0.01°) in the considered impedance and frequency range.

V. Measurements in Ex Vivo Bovine Liver

Once calibration of the measurement system was completed, an experimental test was performed in ex vivo bovine liver, chosen for its good homogeneity compared with other tissues, such as the kidney, pancreas, and muscle. Furthermore, it has a lower stiffness as compared with other tissues: this peculiarity allows an easy needle electrode insertion inside the liver. In addition, it has a good ease of processing, allowing to cut tissue samples with the desired shape and size, to make them well-matched with the plastic box used as a sample holder, whose dimensions have been selected in Section II-B. Fig. 8 displays the compact measurement system setup.

Starting from two different bovine livers, dielectric measurements were carried out on six tissue samples obtained from them. The livers were bought at a butcher shop within three days from the butchery, and the samples were prepared, discarding any parts with large blood vessels, to prevent measurement artifacts owing to the presence of air within.

Measurements on three samples of the same liver were carried out over three consecutive days, during which samples have been preserved in a freezer, and, before beginning the measurement session, they have been placed at room temperature for 8 h to achieve temperature stabilization. Overall, therefore, measurements were performed in six samples of bovine liver. In this way, it was possible to verify the repeatability of the experimental data, by carrying out ten repeated measurements in the same sample at each desired frequency, and their reproducibility, performing measurements both in different samples from the same liver and in livers from different animals.

At the frequencies of interest ($\leq$1 kHz), it can be argued that the circuit model of biological tissues can be represented as a parallel *RC* [35]. From the measurement of the impedance magnitude and phase, it is possible to obtain, by way of a custom program developed in LabVIEW, the conductance (G) and the susceptance (B) of the tissue, which are directly related to the conductivity and relative permittivity, respectively, through (1) and (2), where f is the measurement frequency and $k = (0.09706 \pm 0.00016)$ m, as found from the calibration.

Two different measurement methods were tested for evaluating the dielectric properties of the bovine liver at the frequencies of interest. In the first method, ten repeated measurements ($N = 10$) were carried out for each of the considered frequencies (i.e., 0.1 Hz, 1 Hz, 100 Hz, and 1 kHz) to obtain the corresponding values of conductance (G) and susceptance (B), that is the same method used for calibration in standard saline solutions. In the second method, the conductance (G) and the susceptance (B) were measured at the five considered frequencies for each repeated measurement ($N = 10$). Moreover, the conductivity values can be classified, for each measurement frequency, according to the average measured temperature, thus obtaining the conductivity behavior as a function of temperature. Fig. 9 shows the regression curve of measured conductivity as a function of temperature, at 0.1 Hz for one of the considered liver samples; data were obtained by using the second measurement method, which considerably limits the effect of temperature increase during measurements.

It is worth noting here that the error bars in Fig. 9 are not shown as they would not be visible, since the relative uncertainty is about 1%.

Conductivity measurement results are shown in Fig. 10 in the range of 0.1–1000 Hz; they show a constant behavior as a function of frequency. Data are compared with results taken from the literature [18], [20]. The black dashed line in Fig. 10 depicts the average of the mean conductivities computed for the different samples. Its frequency variability is lower than 10%. The literature comparisons highlight a reasonable agreement with the study of Wang et al. [20].

The undesirable effects due to temperature variations ($\leq$2 °C) are limited, since the trend appears constant in the considered frequency range. These observations point out that the presented method presents clear advantages for the measurement of the conductivity at very low frequency.

In addition, ex vivo experiments have been carried out in bulk bovine liver resulting in measured values of conductivity

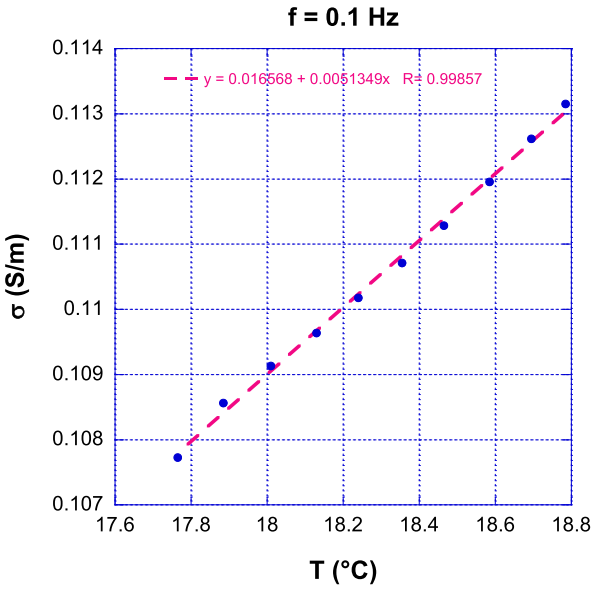

Fig. 9. Behavior of the conductivity as a function of liver temperature and the related regression line.

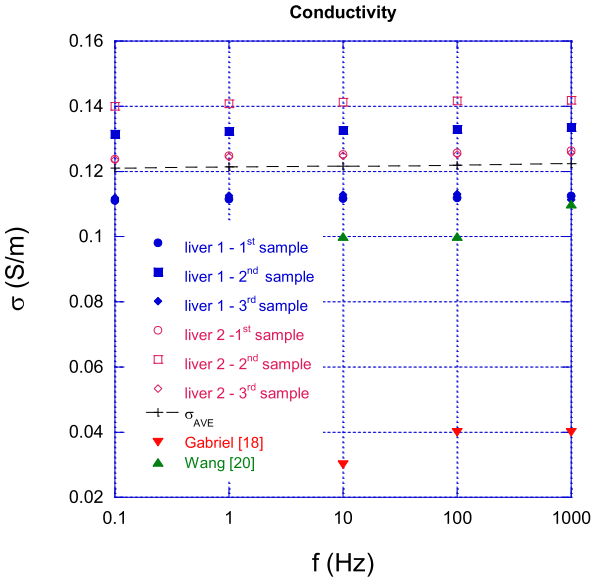

Fig. 10. Behavior of the average conductivity as a function of frequency. Data are compared with those of [18] and [20].

very similar to those achieved from samples of the same liver tissue, cut in such a way as to fill a plastic holder. The conductivity variation was within 5%, partly justified by the temperature difference of the two samples, which differed by about 8 °C during the experiments. This leads to the conclusion that the geometrical configuration of the measurement system, with the sample placed inside the container, does not significantly influence measurement results.

As for the relative permittivity, the observed measured value dispersion was quite high at the lower frequencies; in particular, at 0.1- and 1-Hz measurement, variations up to 65% were assessed. Instead, at frequencies greater than or equal to 10 Hz, more repeatable results were obtained with variations in measured values within 10%. This effect is an index that the permittivity measurements at ultralow frequency are greatly affected by noise. However, the complex permittivity, given

by $\varepsilon_c = \varepsilon' - j\varepsilon'' = \varepsilon' - j\sigma/\omega\varepsilon_0$, at the very low frequencies is completely dominated by the imaginary part [18]; therefore, the parameter of interest is the conductivity, that is well characterized by the presented system. As an example, considering ε' and ε'' of body tissues computed at 0.1 Hz using the tool available in [36], we obtained the $\varepsilon''/\varepsilon'$ ratio of about 120 for liver tissue and of about 1000 for muscle. Higher ratios are obtained for other biological tissues, thus highlighting the prominent effect of the imaginary part.

VI. Conclusion

In this article, a compact and low-cost system for measuring dielectric properties of biological tissues is presented. In particular, the frequencies of interest are the extremely low and ultralow frequencies, i.e., the range between 0.1 Hz and 1 kHz. To retrieve the tissue samples' complex permittivity, first, the system was calibrated in physiological solutions: in this way, the cell constant k was obtained. Subsequently, dielectric measurements were carried out in six tissue samples, got from two different livers.

Comparisons with data from the literature show that the conductivity values are similar to those of Wang et al.'s [20] research work. In fact, a similar four-electrode measurement system was used in that paper. In contrast, differences with Gabriel's data [30] can be ascribed to the use of an open-ended coaxial probe. This type of sensor is known to suffer from reduced accuracy at low frequency.

The presented measurement method has obvious advantages for the conductivity measurement at ELF and ULF frequencies, with a low-temperature effect; while for evaluating permittivity, the proposed system is efficient for frequencies greater than or equal to 10 Hz, where the complex permittivity is no longer dominated by conductance.

As regards future developments, studies will be devoted to the enhancement of the system compactness. In particular, to achieve a more efficient solution, the DAQ board will be substituted by a suitable microcontroller. This will allow not only to make the measurement system as small as possible but also to reduce system costs. In addition, the design of the system will be enhanced, for example, designing a more compact arrangement of the electrodes, allowing the use of smaller tissue samples.

As highlighted in the introduction, the problem of knowing the electrical properties of biological tissues at very low frequency acquires relevance if specific exposure scenarios are taken into consideration, such as that of healthcare personnel operating on MRI systems (given that the situation of an operator in proximity to an MR imaging device can be compared with that of a stationary subject in a homogeneous magnetic field slowly varying over time); in addition, knowledge of the dielectric properties of tissues at frequencies below 10 Hz is important for electroporation, electrochemotherapy, and numerical dosimetry; therefore, possible uses of the proposed system are related to all these application fields.

References

[1] J. Frankel, J. Wilén, and K. Hansson Mild, "Assessing exposures to magnetic resonance Imaging's complex mixture of magnetic fields for in vivo, in vitro, and epidemiologic studies of health effects for staff and patients," *Frontiers Public Health*, vol. 6, Mar. 2018, Art. no. 313433, doi: 10.3389/fpubh.2018.00066.

[2] J. Bonello and C. V. Sammut, "Experimental analysis of radiographer exposure to the static field from a 1.5-T magnetic resonance imaging machine," *Int. J. Occupational Saf. Ergonom.*, vol. 23, no. 1, pp. 133–138, Jan. 2017, doi: 10.1080/10803548.2016.1216357.

[3] D. Andreuccetti et al., "Numerical assessment of induced current density due to occupational exposure to magnetic resonance gradient fields," in *Proc. 9th Int. Congr. Eur. Bioelectromagn. Assoc. (EBEA)*, Rome, Italy, Feb. 2011.

[4] Y. Lv, C. Yao, and B. Rubinsky, "A 2-D cell layer study on synergistic combinations of high-voltage and low-voltage irreversible electroporation pulses," *IEEE Trans. Biomed. Eng.*, vol. 67, no. 4, pp. 957–965, Apr. 2020, doi: 10.1109/TBME.2019.2925774.

[5] H. Cindric et al., "Retrospective study for validation and improvement of numerical treatment planning of irreversible electroporation ablation for treatment of liver tumors," *IEEE Trans. Biomed. Eng.*, vol. 68, no. 12, pp. 3513–3524, Dec. 2021, doi: 10.1109/TBME.2021.3075772.

[6] A. Tamra, A. Zedek, M.-P. Rols, D. Dubuc, and K. Grenier, "Single cell microwave biosensor for monitoring cellular response to electrochemotherapy," *IEEE Trans. Biomed. Eng.*, vol. 69, no. 11, pp. 3407–3414, Nov. 2022, doi: 10.1109/TBME.2022.3170267.

[7] I. Lackovic, R. Magjarevic, and D. Miklavcic, "Three-dimensional finite-element analysis of Joule heating in electrochemotherapy and in vivo gene electrotransfer," *IEEE Trans. Dielectr. Electr. Insul.*, vol. 16, no. 5, pp. 1338–1347, Oct. 2009, doi: 10.1109/TDEI.2009.5293947.

[8] M. Pavlin et al., "Effect of cell electroporation on the conductivity of a cell suspension," *Biophys. J.*, vol. 88, no. 6, pp. 4378–4390, Jun. 2005.

[9] A. Silve, R. Vezinet, and L. M. Mir, "Nanosecond-duration electric pulse delivery in vitro and in vivo: Experimental considerations," *IEEE Trans. Instrum. Meas.*, vol. 61, no. 7, pp. 1945–1954, Jul. 2012, doi: 10.1109/TIM.2012.2182861.

[10] M. Cavagnaro, S. Pisa, and E. Pittella, "Safety aspects of people exposed to ultra wideband radar fields," *Int. J. Antennas Propag.*, vol. 2013, no. 1, 2013, Art. no. 291064, doi: 10.1155/2013/291064.

[11] (2007). *The World Health Report 2007: A Safer Future: Global Public Health Security in the 21st Century*. Accessed: Jun. 18, 2024. [Online]. Available: https://www.who.int/publications/i/item/9789241563444

[12] ICNIRP, "Guidelines for limiting exposure to time-varying electric and magnetic fields (1 Hz to 100 kHz)," *Health Phys.*, vol. 99, no. 6, pp. 818–836, 2010.

[13] H. P. Schwan, "Electrical properties of tissue and cell suspensions," *Adv. Biol. Med. Phys.*, vol. 5, pp. 147–209, Jan. 1957.

[14] F. X. Hart, "Some precautions in the use of time-domain dielectric spectroscopy with biological and other lossy dielectrics," *Med. Biol. Eng. Comput.*, vol. 20, no. 4, pp. 401–407, Jul. 1982.

[15] F. X. Hart, "The extremely low frequency electrical properties of plant stems," *Bioelectromagnetics*, vol. 6, no. 3, pp. 243–256, Jan. 1985.

[16] K. R. Foster and H. P. Schwan, "Dielectric properties of tissues and biological materials: A critical review," *Crit. Rev. Biomed. Eng.*, vol. 17, no. 1, pp. 25–104, 1989.

[17] B. Singh, C. W. Smith, and R. Hughes, "In vivo dielectric spectrometer," *Med. Biol. Eng. Comput.*, vol. 17, no. 1, pp. 45–60, Jan. 1979.

[18] S. Gabriel, R. W. Lau, and C. Gabriel, "The dielectric properties of biological tissues: II. Measurements in the frequency range 10 Hz to 20 GHz," *Phys. Med. Biol.*, vol. 41, no. 11, pp. 2251–2269, 1996.

[19] S. Laufer, A. Ivorra, V. E. Reuter, B. Rubinsky, and S. B. Solomon, "Electrical impedance characterization of normal and cancerous human hepatic tissue," *Physiol. Meas.*, vol. 31, no. 7, pp. 995–1009, Jul. 2010.

[20] H. Wang et al., "Dielectric properties of human liver from 10 Hz to 100 MHz: Normal liver, hepatocellular carcinoma, hepatic fibrosis and liver hemangioma," *Bio-Med. Mater. Eng.*, vol. 24, no. 6, pp. 2725–2732, 2014.

[21] *Alpha-A Modular Dielectric/Impedance Measurement System*. Accessed: Jun. 18, 2024. [Online]. Available: https://www.novocontrol.de/php/ana_alpha_main.php

[22] *Dielectric Spectroscopy, Application Description*. Accessed: Jun. 18, 2024. [Online]. Available: https://www.zhinst.com/europe/en/applications/impedance-measurements/dielectric-spectroscopy

[23] S. Sahoo, "Investigation of dielectric relaxation in dipolar liquids," *Indian J. Phys.*, vol. 94, no. 1, pp. 17–29, Jan. 2020, doi: 10.1007/s12648-019-01437-3.

[24] D. Kumar, S. K. Sit, S. N. Singh, and S. Sahoo, "Dielectric relaxation behavior of amide and phenol mixtures in C_6H_6 under microwave field," *J. Solution Chem.*, vol. 50, no. 5, pp. 690–722, May 2021.

[25] V. Lopresto, S. Pisa, E. Pittella, and E. Piuzzi, "Compact system for measuring the dielectric properties of biological tissues at extremely-low and ultra-low frequencies," in *Proc. IEEE Int. Symp. Med. Meas. Appl. (MeMeA)*, Jun. 2022, pp. 1–6.
[26] X. Zhu et al., "I-V method based PDN impedance measurement technique and associated probe design," in *Proc. IEEE Int. Symp. Electromagn. Compat., Signal Power Integrity (EMC+SIPI)*, New Orleans, LA, USA, Jul. 2019, pp. 30–33, doi: 10.1109/ISEMC.2019.8825297.
[27] D. K. Swanson and J. G. Webster, "Errors in four-electrode impedance plethysmography," *Med. Biol. Eng. Comput.*, vol. 21, no. 6, pp. 674–680, Nov. 1983, doi: 10.1007/bf02464029.
[28] L. D'Alvia et al., "Tetrapolar low-cost systems for thoracic impedance plethysmography," in *Proc. IEEE Int. Symp. Med. Meas. Appl. (MeMeA)*, Jun. 2018, pp. 1–6, doi: 10.1109/MEMEA.2018.8438663.
[29] I. V. Lam, "Analysis of improved howland current pump configurations," Appl. Note, Feb. 2023.
[30] C. Gabriel, A. Peyman, and E. H. Grant, "Electrical conductivity of tissue at frequencies below 1 MHz," *Phys. Med. Biol.*, vol. 54, no. 16, pp. 4863–4878, Aug. 2009.
[31] Radwag AS 220.Y model, *Datasheet AS R Analytical Balances*. Accessed: Jun. 18, 2024. [Online]. Available: https://radwag.com/it/mas-220-y-modulo-di-pesatura,w1,2FA,116-115-100#5
[32] *Handheld Thermometers*. Accessed: Jun. 18, 2024. [Online]. Available: https://www.transcat.com/media/pdf/1521t_1522t.pdf
[33] *Delta OHM HD 2106.1, HD 2106.2 Conductivity Meters—Thermometers*, Delta OHM, , Rev. 1.2, Mar. 2023.
[34] R. H. Shreiner and K. W. Pratt, "Primary standards and standard reference materials for electrolytic conductivity," NIST, Gaithersburg, MD, USA, Tech. Rep. 260-142, 2004.
[35] D. A. Dean, T. Ramanathan, D. Machado, and R. Sundararajan, "Electrical impedance spectroscopy study of biological tissues," *J. Electrostatics*, vol. 66, nos. 3–4, pp. 165–177, Mar. 2008, doi: 10.1016/j.elstat.2007.11.005.
[36] *ITIS Foundation, Tissue Properties*. Accessed: Jun. 18, 2024. [Online]. Available: https://itis.swiss/virtual-population/tissue-properties/database/tissue-frequency-chart/

Erika Pittella (Member, IEEE) is an Assistant Professor with the Department of Information Engineering, Electronics and Telecommunications, Sapienza University of Rome, Rome, Italy. In 2014, she was involved as a Tutor in the high-level postgraduate course in aerospace engineering for the TigriSat Satellite Project. She was a Visiting Researcher at King's College London, London, U.K. She has coauthored 70 articles published in international journals and conference proceedings. Her research interests include the measurement of complex permittivity of materials, time-domain reflectometry applications, and biomedical instrumentation design.

Dr. Pittella is a reviewer of several scientific journals, including IEEE TRANSACTIONS ON INSTRUMENTATION AND MEASUREMENT, *Measurement*, *Sensors Journal*, *Sensors*, and IEEE ANTENNAS AND WIRELESS PROPAGATION LETTERS. She is the Treasurer of the IEEE Instrumentation and Measurement Italy Chapter, and a member of the IEEE Instrumentation and Measurement Society, the IEEE Women in Engineering (WIE) Affinity Group (AG), the IEEE Italy Section, and the Electrical and Electronic Measurements Group (GMEE).

Vanni Lopresto is a Senior Research Scientist and a Safety Officer at Italian National Agency for New Technologies, Energy and Sustainable Economic Development (ENEA), Infrastructures and Services Directorate (ISER), Casaccia Research Center, Rome, Italy. He has authored over 80 scientific papers in national and international journals and conferences and is the anonymous referee of peer-reviewed scientific journals. His professional and scientific activity concerns risk assessment, health and safety management, and regulatory compliance for exposure to occupational risks, in particular, to electromagnetic fields.

Dr. Lopresto is a member of the Italian Electrotechnical Committee (CEI) and Technical Committee 106 "Human Exposure to Electromagnetic Fields," the Chair of the Working Group (WG) "Exposure to Electromagnetic Fields from Wireless Power Transfer (WPT) Systems," a member of the European Committee for Electrotechnical Standardization (CENELEC) CLC/TC 106X "Electromagnetic Fields in the Human Environment," WG21 "Basic and General Standards," and a member of the International Electrotechnical Commission (IEC), TC106/WG9 "Addressing methods for Assessment of WPT related to Human Exposures to Electric, Magnetic, and Electromagnetic Fields" and TC106/PT63184 "Human Exposure to Electric and Magnetic Fields from WPT Systems." He has been a Scientific Advisor at the Interforce Operating Group of the Italian Ministry of Inner Affairs for the Experimentation of Electrical Pulses Incapacitating Devices, the Co-Chief Scientific Investigator of the Coordinated Research Project of the International Atomic Energy Agency (IAEA) "Application of Wireless Technologies in Nuclear Power Plant Instrumentation and Control Systems-Evaluation of Electromagnetic Fields from Wireless Technologies in Nuclear Plant," a Scientific Coordinator of the research activity "Effects of High-Intensity Static Magnetic Fields" in the BIOxTREME Research Project financed by the Italian Space Agency (ASI), and an ENEA's Scientific Coordinator of the National Strategic Program "Safety and Health Technologies" funded by Italian Ministry of Health, and of the Italian Industrial Research Project "TAM–Microwave Thermal Ablation" funded by FILAS-Regione Lazio.

Stefano Pisa (Senior Member, IEEE) received the Electronic Engineering and Ph.D. degrees from the University of Rome "La Sapienza," Rome, Italy, in 1985 and 1988, respectively.

In 1989, he joined the Department of Information Engineering, Electronics and Telecommunications (DIET), Sapienza University of Rome, Rome, as a Researcher, where he has been an Associate Professor, since 2001. He has authored over 180 scientific papers. His research interests include the interaction between electromagnetic fields and biological systems, therapeutic and diagnostic applications of electromagnetic fields, medical applications of radar, permittivity measurements and models of materials, and modeling and design of microwave circuits.

Prof. Pisa is a Senior Member of the IEEE Microwave Theory and Techniques Society and the International Union of Radio Science (URSI), and a member of the Italian Society of Electromagnetics (SIEm).

Emanuele Piuzzi (Member, IEEE) received the M.S. (cum laude) and Ph.D. degrees in electronic engineering from Sapienza University of Rome, Rome, Italy, in 1997 and 2001, respectively.

He is currently an Associate Professor in electrical and electronic measurements with the Department of Information Engineering, Electronics and Telecommunications (DIET), Sapienza University of Rome. His current research interests include the measurement of complex permittivity of materials and their application to material characterization and monitoring, biomedical instrumentation design for wearable and remote monitoring applications, and evaluation of human exposure to electromagnetic fields.

Dr. Piuzzi is a member of the Italian Group of Electrical and Electronic Measurements (GMEE) and the Italian Electrotechnical Committee (CEI).

Open Access funding provided by 'Università degli Studi di Roma "La Sapienza" 2'
within the CRUI-CARE Agreement